

Time-resolved MRA with Data-Driven Parallel Imaging Using Calibration Over Multiple Time-Frames and Interleaved Variable Density Cartesian Acquisition

J. H. Holmes¹, K. Wang², P. J. Beatty³, R. F. Busse⁴, F. R. Korosec⁵, L. A. Keith², C. J. Francois⁶, S. B. Reeder⁵, and J. H. Brittain⁷

¹Global Applied Science Laboratory, GE Healthcare, Madison, WI, United States, ²Medical Physics, University of Wisconsin-Madison, Madison, WI, ³Global Applied Science Laboratory, GE Healthcare, Thornhill, ON, Canada, ⁴MR Research, GE Healthcare, Waukesha, WI, ⁵Radiology, University of Wisconsin-Madison, Madison, WI, ⁶Radiology, University of Wisconsin-Madison, Madison, WI, ⁷Global Applied Science Laboratory, GE Healthcare, Madison, WI

Introduction: Use of an Interleaved Variable Density (IVD) sampling pattern combined with multiplicative constrained reconstruction (HYCR) can provide significant acceleration for time-resolved MRA [1-3]. Further, this sampling pattern can be combined with regular undersampling and data-driven parallel imaging (DDPI) [4]. DDPI using multiple sources of calibration data has been demonstrated for cases where only limited data is available or motion is present [5,6]. The IVD sampling scheme provides flexibility to calibrate using multiple datasets including the pre-contrast mask and data from within each time-frame. Calibration on the mask data provides benefits in that the time-frames can be further accelerated, however the mask data is considerably less sparse and is inconsistent with the accelerated data since it is acquired pre-contrast. Internal calibration (autocalibration) provides improved sparsity however this comes with a tradeoff in terms of the achievable temporal frame-rate. In this work we present results from calibrating using data acquired during the pre-contrast mask, during the time-frame itself, and we demonstrate a novel method to maintain high frame rates using a combination of calibration data from multiple time-frames optimizing on high temporal resolution.

Methods: Peripheral run-off studies were performed in normal volunteers on a 3 T MRI system (MR750, GE Healthcare, Waukesha, WI), using a 32 channel phased array coil (NeoCoil, Waukesha, WI). The IVD-HYCR acquisition was performed with the phase encodes in the axial plane and parameters included elliptical centric view ordering, 48 (S/I) \times 33.6 (R/L) \times 12.9 (A/P) cm^3 FOV, 512 (freq) \times 360 (phase) \times 68 (slice) acquired matrix for an acquired resolution of $0.94 \times 0.94 \times 1.9 \text{ mm}^3$, and update time 7.5 s with the center of k-space sampled during each frame. Parallel imaging acceleration of 4x (2x in both the y and z directions) was performed and the sampling pattern from a single time-frame is shown in Fig. 1. Calibration for DDPI was performed on 3 different datasets: the pre-contrast mask, the mask-subtracted time-frame, and a combination of the current and four future mask-subtracted time-frame. Calibration on the mask data was performed over a 30x30 central region using a 3x7x7 kernel. Regions of 20x80 were used from the mask-subtracted time-frames with a kernel width of 3x5x5. In the combination calibration approach, unaliasing coefficients were calculated that were consistent with all of the calibration data sets. Images were zero-filled in the unacquired phase encode locations due to the IVD undersampling. Time-frame images were evaluated for overall noise performance and evidence of coherent aliasing due to the regular undersampling. MIP images in the y-z phase encoding (axial) plane are displayed to more readily show any artifacts due to the parallel imaging.

Results: Calibration on mask-subtracted time-frame data provides advantages in terms of image sparsity however not all aliasing was corrected in regions without signal due to movement of the contrast bolus down the legs resulting in data inconsistency (Fig. 2 a). Calibration on the mask-subtracted time-frame data acquired immediately following the accelerated data provided improved calibration however the aliasing could not be fully removed due to the highly limited amount of calibration data (Fig. 2 b). Three time-frames reconstructed using internal calibration data showed very little incoherent noise however there were significant aliasing artifacts still visible (Fig. 3 a-c, arrows) due to the limited amount of calibration data acquired to maintain high temporal resolution. Calibration data taken from the pre-contrast mask effectively removed the coherent aliasing as a significantly greater amount of calibration data is available but there is greater overall noise in each time-frame (Fig. 3 d-f, arrows). Calibration performed on smaller regions of the mask data was not found to be sufficient to remove the coherent aliasing. The combination calibration data from multiple mask-subtracted time-frames was found to provide a sufficient amount of calibration data that is more consistent with the accelerated data to remove the coherent aliasing as well as decrease the incoherent noise (Fig. 3 h-j).

Discussion: The IVD sampling scheme combined with parallel imaging and HYCR provides flexibility in selection of data for calibration. In this work we have compared calibration on the mask data, mask-subtracted data from specific time-frames, and a combination calibration using multiple mask-subtracted time-frames. While the mask data is much less sparse, it does allow removal of aliasing over all regions of the legs that have pre-contrast signal. The combination calibration method was found to provide better unaliasing and overall image quality. Due to the elliptical centric view ordering, there is time for movement of the contrast bolus down the arteries between the time-frame calibration data and the later portions of the accelerated time-frame data. The combination calibration approach provides advantages in terms of temporal resolution as well as mitigation of artifacts due to parallel imaging.

References: [1] Busse et al. ISMRM 2009; A4534. [2] Busse et al. ISMRM 2009; A2834. [3] Wang et al. ISMRM 2009; A3884. [4] Wang et al. ISMRM 2010; A352. [5] Beatty et al. ISMRM 2008; A1464. [6] Brau et al. ISMRM 2008; A1300.

Figure 1. IVD sampling pattern in the phase encode (axial) plane for a single time-frame. Sampled points are shown in white.

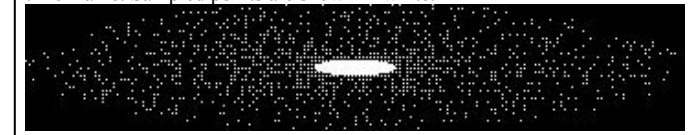


Figure 2. Arterial phase coronal and axial MIPs of the calves reconstructing an n^{th} time-frame with calibration performed using mask-subtracted data from different individual time-frames. Note reduced coherent aliasing as calibration data that is more consistent with the accelerated data within the n^{th} time-frame is used, due to movement of the contrast bolus (a-c, arrows). With elliptical centric view ordering, the $n+1$ frame provides calibration data acquired immediately following the accelerated data to better capture spatial locations occupied by the contrast bolus during acquisition of the accelerated data (c).

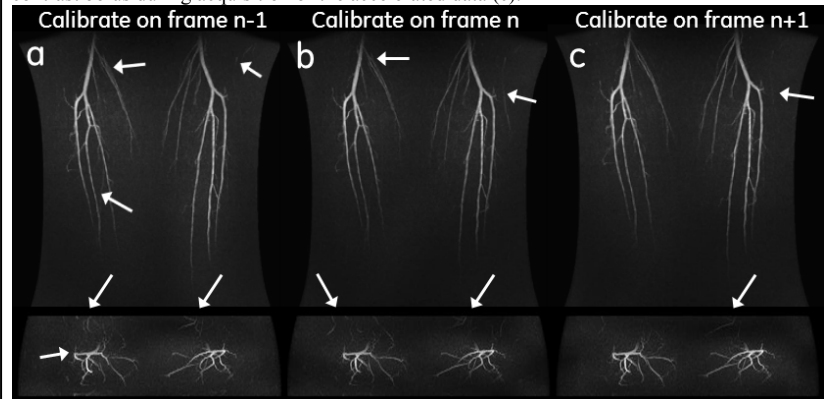


Figure 3. Axial MIPs in the undersampled phase encode plane of 3 time-frames during the arterial phase. Residual coherent aliasing is visible in the images using internal calibration data (a-c, arrows). There is greater noise visible in the images using calibration from the mask data although no coherent aliasing is visible (d-f, arrows). Combining calibration data from multiple mask-subtracted time-frames allows for effective removal of the coherent aliasing as well as overall higher image quality (h-j). Images are individually windowed and leveled.

